Polyelectrolyte Counterion Condensation Theory Explains Differential Scanning Calorimetry Studies of Salt-Induced Condensation of Chicken Erythrocyte Chromatin†

R. Labarbe, S. Flock, C. Maus, and C. Houssier*

Laboratoire de Chimie Macromoléculaire et Chimie Physique, Institut de Chimie, Université de Liège B-4000 Liège, Belgium

Received July 18, 1995; Revised Manuscript Received October 25, 1995⊗

ABSTRACT: The salt-induced chromatin condensation in chicken erythrocyte nuclei is studied by differential scanning calorimetry (DSC). The degree of chromatin condensation is measured for condensation induced by monovalent, divalent, trivalent, or tetravalent cations and by a mixture of sodium and magnesium. These last two cations show an evident competition effect. Salt-induced chromatin condensation is shown to be an entropy-driven process. A simple model of chromatin based on the polyelectrolyte counterion condensation theory is used in order to compute the charge neutralized by the cations in each chromatin domain. The degree of chromatin condensation is shown to be related to the weighed sum of the square of the phosphate charge of each domain. The model predicts the salt and the chromatin concentration dependence of the condensation and the effect of H1 removal.

Chromatin adopts different degrees of compaction depending on the cation concentration. An increase of the ionic strength provokes the transition of the fiber from an extended 10 nm fiber to the compact 30 nm fiber [for a review, see Widom (1989)], which was described as a solenoid composed of 6 nucleosomes per turn with a 110-Å pitch (Finch & Klug, 1976) but is now suspected not to be as regular as previously thought (Zlatanova et al., 1994). The folding process was studied by numerous methods, but in most of the techniques, preparative steps, such as chromatin extraction from nuclei for spectroscopy or fixative treatments for electron microscopy or X-ray scattering, perturb the chromatin structure and may cause artifacts. Furthermore, the above methods only afford a measure of an average contraction ratio of the fiber (e.g., by sedimentation analysis or light scattering). Differential scanning calorimetry (DSC)[1] can be used to study the chromatin *in situ* inside nuclei or even inside whole cells (Touchette & Cole, 1985) and offers a direct determination of the proportion of chromatin in different condensation states (Barboro et al., 1993). Nevertheless, probably due to a previous controversy in thermogram interpretation that is now definitely resolved (Cavazza et al., 1991), no extensive study of the effect of salt on chromatin condensation has been carried out by DSC up to now.

It is essential to have some understanding of the physicochemical mechanisms underlying chromatin condensation. The stability of the condensed chromatin structure is the result of two opposing forces: an attractive force due to the formation of interprotein bounds, interactions from the transient dipoles resulting from concentration fluctuations in the counterion atmosphere (Marquet et al., 1991), etc. and an electrostatic repulsive force between the negatively charged phosphate groups. Several authors have already suggested that the main contribution originates from electrostatic interactions (Widom, 1986; Clark & Kimura, 1990; Subirana, 1992). In order to understand the mechanism of the cation−polyelectrolyte interactions, several theories have already been applied to DNA, such as the Monte-Carlo (Le Bret & Zimm, 1984), Poisson-Boltzmann (Jayaram et al., 1989) and Manning (1978) theories. However, treating chromatin in terms of cation−polyelectrolyte interactions is more difficult, as the presence of histones and the complex three-dimensional structure should be taken into account. Manning theory, which is computationally the simplest, could seem the less adequate for treating chromatin because it is, strictly speaking, valid only for an infinitely long line of charges in an infinitely diluted 1:1 salt. However, it was shown that it gives correct results for finite length polyelectrolyte (Fenley et al., 1990), curved line charges, and helical line charges (Fenley et al., 1992) in the presence of DNA−protein contact (Manning et al., 1989) and that under certain conditions it is equivalent to the theoretically more correct Poisson-Boltzmann theory (Fogolari et al., 1993; Rajasekaran & Jayaram, 1994). Widom (1986) showed that chromatin condensation can be qualitatively interpreted in terms of Manning theory. In a very interesting quantitative treatment, Clark and Kimura (1990) showed the existence of a relationship between the degree of chromatin condensation and the electrostatic free energy of DNA. However, there were limitations to their theoretical approach because they computed the electrostatic free energy by treating chromatin as a line of charges and they took into account DNA neutralization by the different histones through a global neutralization factor. We propose here a more detailed chromatin model that overtakes those limitations. The nucleosomal DNA is divided in three domains: linker, linker neutralized by H1, and core particle. The amount of counterion condensed around DNA is then computed separately in each domain according to Manning's theory, which is thus applied locally (and not to the whole chromatin) and with a different histone

† Supported by the Fonds National de la Recherche Scientifique of Belgium (FNRS fellowship to R.L.), FRIA (research fellowship to S.F.), and research Grants FRFC 2/4501/91, FNRS-Télévie 7/4526/95, and ARC 91/95-152.

⊗ Abstract published in *Advance ACS Abstracts,* February 1, 1996.

[1] Abbreviations: DSC, differential scanning calorimetry; DM, dissociation medium; EDTA, ethylenediaminetetracetic acid; PMSF, phenylmethanesulfonyl fluoride.

0006-2960/96/0435-3319$12.00/0 © 1996 American Chemical Society

neutralization factor for each domain. As the interdomain distances are sufficiently large, each domain can be treated separately. The electrostatic energy is the sum of the electrostatic repulsions between the residual phosphate charges of each domain.

EXPERIMENTAL PROCEDURES

Preparation of Chicken Erythrocyte Nuclei. Blood was collected from freshly killed chickens, filtered on cheesecloth, and dissolved in 1.5 vol of citrate buffer (0.76% sodium citrate, 1% D-glucose, 0.5 mM PMSF, pH 7.4). The solution was centrifuged at 900*g* for 20 min. The pellet was repeatedly washed with DM (75 mM NaCl, 24 mM Na_2-EDTA, 5 mM $NaHSO_3$, 1 mM PMSF, pH 7.8) containing 0.5% (v/v) Triton X-100 and then centrifuged at 5000*g* for 15 min until the pellet was totally white. The pellet was then washed at least three times with DM, under the same conditions, and resuspended in DM containing 50% (v/v) of glycerol. The nuclei can be kept in this solution at −20 °C for several months. The pellets were washed three times with buffers containing sodium cacodylate (pH 6.5) and the required salt concentration. They were equilibrated for 20 min in the buffer and then centrifuged at 4000*g* for 10 min. The samples (about 15 mg) were then sealed in a small volume (20 μL) aluminium DSC pan.

Calorimetry. The DSC experiments were performed on a Solomat 4000 at a scanning rate of 10 °C/min. The thermograms were recorded on a personal computer directly connected to the calorimeter. The heat capacity was computed from the heat flow using a program furnished by the Solomat Company (Stamford, CT). A linear baseline was subtracted from the heat capacity versus temperature thermogram, which is then numerically deconvoluted by fitting a sum of Gaussian curves using a Marquardt-Levenberg algorithm. To determine the DNA concentration, the sample was dissolved in 1 mol/L NaOH, and the absorbance of the solution was measured at 260 nm (ϵ = 11 000 cm M^{-1}). This simple and widely used method (Butler, 1980; Thomas & Khabaza, 1980; Bates et al., 1981; Thomas & Rees, 1983) was shown to be very reliable (Russo et al., 1995).

Resolution of Manning Equations. The solutions of the Manning eqs were computed numerically using a modified Marquardt-Levenberg algorithm. The phosphate concentration in the chromatin solution was equal to 10^{-3} M in the calculations.

RESULTS

In a typical thermogram of chicken erythrocyte nuclei (Figure 1), three main endotherms are observed around 80 °C [labeled III by Balbi et al. (1989)], 90 °C (labeled IV), and 107 °C (labeled Va) that are attributed unambiguously to the denaturation of linker DNA, of core particle DNA in extended structure, and of core particle DNA for core particles interacting in condensed structures, respectively [for a review, see Balbi et al. (1989) and Cavazza et al. (1991)]. The number of endotherms can be determined by simple visual inspection. Obviously, an increase of the number of Gaussian components would improve the fit quality, but no physical interpretation can be attributed to the supplementary Gaussians. The deconvolution of the thermograms with the minimum number of endotherms is unique, and the parameters are precisely defined as indicated by the small confidence interval for the temperature in most cases and a confidence interval of 5% for the relative area of the endotherms. The reproducibility and the accuracy of the DSC experiments were tested by repeating some experiments six times as shown in Figure 1B. The experimental standard deviation of the DSC curves is 5%. The DSC thermogram is very sensitive to any DNA digestion. Barboro et al. (1993) have shown that the minimal chain length that gives a DSC signal at 107 °C is 2 kilobase pairs. The preparation procedure using DM buffer is known to give intact high molecular weight chromatin in a state very similar to that found in whole nuclei and nondegraded histones as already extensively shown by polyacrylamide and agarose gel electrophoresis (Balbi et al., 1989; Cavazza et al., 1991; Russo et al., 1995).

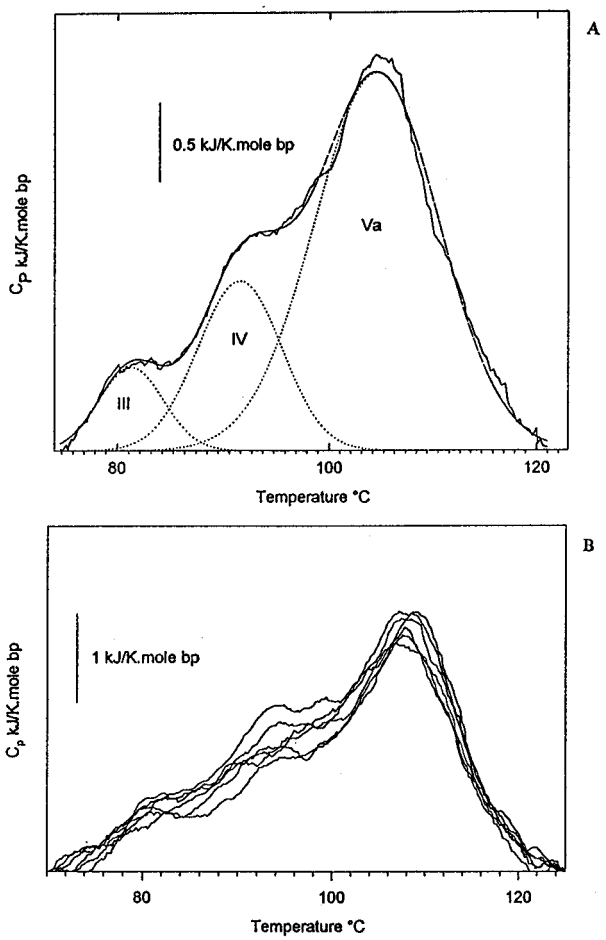

FIGURE 1: (A) Differential scanning calorimetry thermogram of chicken erythrocyte nuclei in the presence of 150 mM NaCl and 600 μM $MgCl_2$. The continuous line is the experimental profile, the dotted lines are the deconvoluted Gaussian endotherms, and the dashed line is the sum of the Gaussian endotherms. (B) DSC thermograms of six samples of chicken erythrocytes nuclei in 150 mM NaCl.

Dependence of Endotherm Temperature on Ionic Strength. The temperature of transition III in chicken erythrocyte chromatin is higher than that reported by other authors for rat hepatocytes (Barboro et al., 1993), calf thymus (Cavazza et al., 1991), and HeLa cells (Touchette & Cole, 1992), indicating that the linker DNA is more stable toward thermal denaturation in chicken erythrocyte than in other chromatin types. The partial replacement of histone H1 by the H5 variant in avian erythroid cells, which is known to bind more

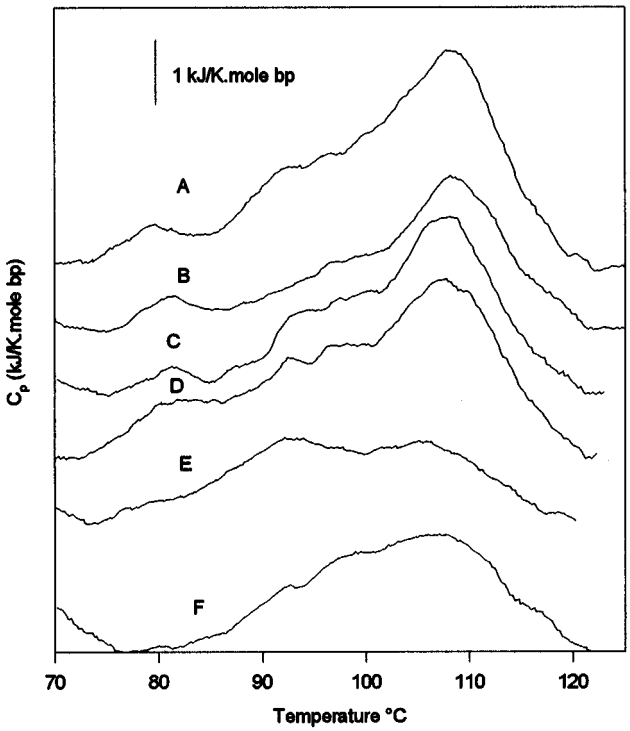

FIGURE 2: Differential scanning calorimetry thermograms of chicken erythrocyte nuclei in DM buffer in the presence of NaCl (A) 150, (B) 120, (C) 80, (D) 60, (E) 40, and (F) 20 mM.

tightly to long DNA fragments (Kumar & Walker, 1980; Thomas & Rees, 1983) than H1 and is supposed to be responsible for the stability of the highly condensed state of chicken erythrocyte chromatin (Bates et al., 1981), results in an increase of the thermal stability of the linker DNA. The linker histone will have few effects on the thermal stability of the core DNA as it is already mainly stabilized by the core histones, leaving T_{IV} and T_{Va} unchanged.

The evolution of chicken erythrocyte nuclei thermograms as a function of sodium chloride concentration is shown in Figure 2. The variations of the temperature of endotherms IV and Va as a function of the concentration of different cations are shown in Figure 3. The slope of the regression lines passing through the points is not statistically different from zero [for details about the statistical test, see Himmelblau (1970)], and thus the temperature of transitions IV and Va are independent of the cation concentration. As a consequence, the chromatin can be considered, from a thermochemical point of view, as a two-state linear system undergoing change from a decondensed state to a condensed state.

Dependence of Endotherm Enthalpy on Ionic Strength. The total denaturation enthalpy ($\Delta H_T = \Delta H_{III} + \Delta H_{IV} + \Delta H_V$) of DNA in chromatin is not dependent on the salt concentration and is equal to $\Delta H_T = 26 \pm 4$ kcal/mole nucleotides. In order to study chromatin condensation, the relative area of transitions IV and Va is determined rather than their absolute enthalpy, this reduces the experimental error due to the knowledge of the total amount of DNA present in the DSC pan.

As the sodium concentration decreases, the area of peak Va decreases relatively to peak IV, leading at low salt concentration to a broad band with poorly resolved peaks (Figure 2). The variations of the relative areas of transitions IV and Va with cation concentration are reported in Figure 3 (left panels). When the sodium concentration increases from 60 to 80 mM, the areas of endotherms IV and Va change from 45% of the total surface each to 30% and 60%, respectively, as a result of chromatin condensation, and the relative surface of endotherm III, which is only a small fraction of total enthalpy, is relatively independent of ionic strength (Figure 3A). Any loss of enthalpy in endotherm IV is compensated for by a proportional increase of endotherm Va (i.e., $\Delta H_{IV} + \Delta H_V =$ constant), indicating that the condensation process is entropy driven ($\Delta H_{cond} = 0$). The same effect is observed with cations of higher charge. The divalent cations calcium and magnesium induce condensation when their concentrations are greater than 150 μM (Figure 3B,C), the trivalent cations terbium and spermidine^{3+} induce condensation when their concentrations are above 75 μM (Figure 3D,E), and the tetravalent spermine^{4+} induces condensation when its concentration is above 30 μM (Figure 3F). This suggests two remarks in agreement with Manning theory: first, the greater the cation charge, the smaller the concentration required to induce condensation; second, the final value of the degree of condensation and the cation concentration inducing condensation are independent of the nature of the cation and depend only on its electrical charge (compare Figure 3, parts D and E, where the difference between the concentrations inducing condensation is at most 10 μM). On the contrary, it was reported that precipitation of 50% DNA requires twice as much spermidine^{3+} as Tb^{3+} (which is significantly different from what is observed here) because exclusion volume effects due to the larger size of the spermidine^{3+} molecule diminish the phosphate neutralization degree (Flock et al., 1995). However, in chromatin, the phosphate groups are neutralized nearly at 50% by the histones, and thus the impact of counterions on condensation is greatly reduced, explaining the observed insignificant difference between the two trivalent cations. Marquet et al. (1988) also observed that the Tb^{3+} concentration needed to induced 50% precipitation of chicken erythrocyte chromatin is twice the corresponding spermidine^{3+} concentration. The lower efficiency of Tb^{3+} for chromatin precipitation than for chromatin condensation has already been reported and explained by its affinity for the N-7 of guanine (Marquet et al., 1988).

The invariance of the temperature and of the total enthalpy with salt concentration indicates that chromatin condensation is a linear process. The enthalpy of endotherm Va is proportional to the amount of condensed chromatin and the sum $\Delta H_{Va} + \Delta H_{IV}$ is proportional to the total amount of chromatin in the nuclei. The condensation ratio *d*

$$d = \frac{\Delta H_{Va}}{\Delta H_{IV} + \Delta H_{Va}} \quad (1)$$

represents the proportion of condensed chromatin in the nucleus. Figure 4 collects data relative to the sodium−magnesium competition experiments. When the magnesium concentration is below 200 μM (Figure 4A,B), an increase of the sodium concentration over 80 mM changes the condensation ratio *d* from 60% (a value that is higher than at 0 μM $MgCl_2$, indicating that the presence of a small magnesium concentration causes a partial condensation of chromatin) to 80%. At 200 μM magnesium (see Figure 5 for thermograms), an increase of sodium concentration from 1 mM (where the chromatin is totally condensed; $d = 80\%$,

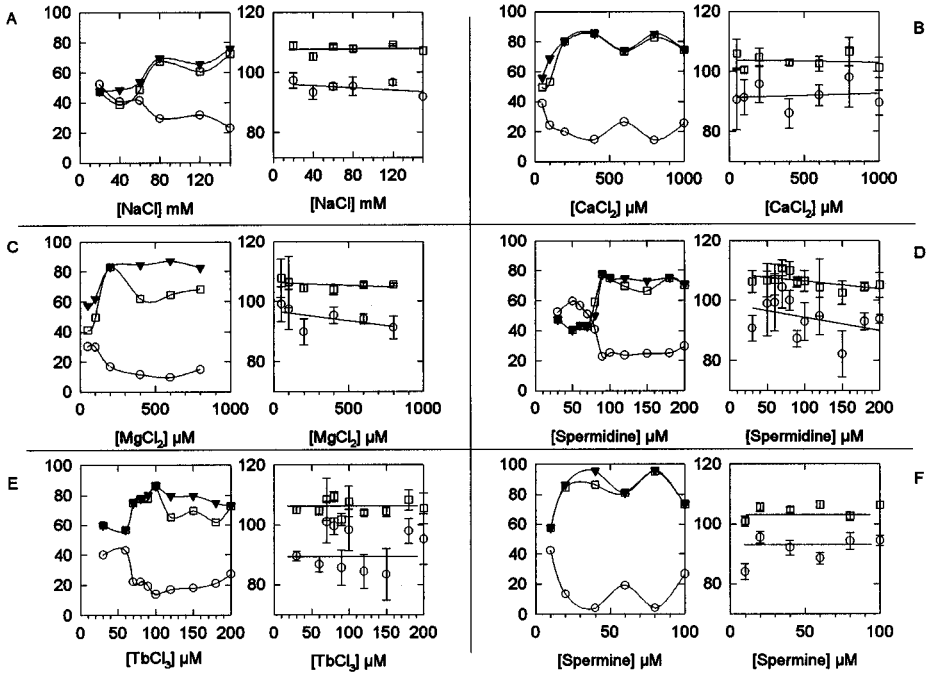

FIGURE 3: Evolution of the peak temperature (°C, right panels) and relative area (%, left panels) of the deconvoluted Gaussian endotherms of DSC thermograms of chicken erythrocyte nuclei as a function of cations concentration: (A) NaCl, (B) $CaCl_2$, (C) $MgCl_2$, (D) spermidine^{3+}, (E) $TbCl_3$, and (F) spermine^{4+}. Circles: endotherm IV; squares: endotherm Va; triangles: condensation ratio (d). Vertical bars are the confidence intervals on the temperature parameter.

Figure 4C) to 80 mM induces chromatin decondensation. A further increase in sodium concentration provokes chromatin recondensation, indicating a clear competition between sodium and magnesium cations, in agreement with Manning theory and with the sodium−magnesium phase diagram drawn by Widom (1986). Above 400 μM, chromatin is totally condensed at any sodium concentrations (Figure 4D−G), and the addition of sodium has nearly no effect on the degree of chromatin condensation. It can be concluded that a condensation ratio d of 50% is characteristic of decondensed chicken erythrocyte chromatin and that $d = 80\%$ is characteristic of the condensed state. Thus, the so-called decondensed chromatin in the nuclei is not totally extended as it still has 50% of its structure that melts in endotherm Va: there are already some interactions between nucleosomes, in agreement with the results of the scanning force microscope experiments of Zlatanova et al. (1994), who showed that even in the absence of salt the fiber is organized in a three-dimensional array of nucleosomes. In the case of calf thymus chromatin, the condensation ratio of the decondensed and condensed states are respectively 25% and 65% (Cavazza et al., 1991). Thus, calf thymus chromatin is less condensed than chicken erythrocyte chromatin, probably because of the absence of H5 histones in the former.

DISCUSSION

Modeling of Chromatin Condensation. Chromatin condensation is modeled as a two-state equilibrium between a condensed and a decondensed state even if it has been reported not to be precisely the case. For example, DSC experiments (Cavazza et al., 1991) show that uncondensed chromatin (ΔH_{IV}) is transformed in about 20 min into a condensed state (ΔH_{Va}) by passing transiently through a semicondensed intermediate (revealed by an endotherm ΔH_{Vb} at 100 °C). However, the kinetic intermediate does not have to be taken into account in the theoretical thermodynamic model, provided the DSC measurements are carried out at the thermodynamical equilibrium by equilibrating the nuclei with the buffer during 20 min before measurements. The counterion atmospheres of both condensed and decondensed states are assumed to contain the same number of counterions. This assumption is correct if (1) DNA bending does not cause a change in the amount of "bound" cations, which was shown previously to be the case (Fenley et al., 1992); (2) when two DNA molecules are brought close together, there is no mutual perturbation of their counterion atmospheres, which is the case for distances greater than the radius of the Manning condensation volume, i.e., approximately 1.4 nm. The equilibrium is characterized by a Gibbs free energy ΔG°_{Cond} per nucleotide:

$$\Delta G^\circ_{Cond} = -kT \ln\left(\frac{d}{1-d}\right) = \Delta G^\circ_{Ionic} + \Delta G^\circ_{Nonionic} \quad (2)$$

The ΔG°_{Ionic} term depends on the amount of counterions near the polyelectrolyte. The $\Delta G^\circ_{Nonionic}$ term, independent of the amount of counterions localized near the polyelectrolyte, takes into account all the contributions to the free energy that are not due to the electrostatic repulsion between phosphate groups. As salt-induced chromatin condensation is essentially an electrostatic process (see above), the variation of $\Delta G^\circ_{Nonionic}$ with cation concentration is negligible with respect to the variation of ΔG°_{Ionic}, and the second term will thus be supposed to be constant in future discussion.

DNA in chromatin is modeled as being divided into three domains. Domain I is linker DNA, free of contact with histones and containing N_I nucleotides. As it is located inside the condensed fiber (Zlatanova et al., 1994; Bartolomé et al., 1994; Labarbe et al., 1996), contacts between DNA and non-histone proteins are unlikely; hence, the fraction of phosphate charges neutralized by the proteins is $\theta_I = 0$. Domain II is the part of linker DNA, containing N_{II}

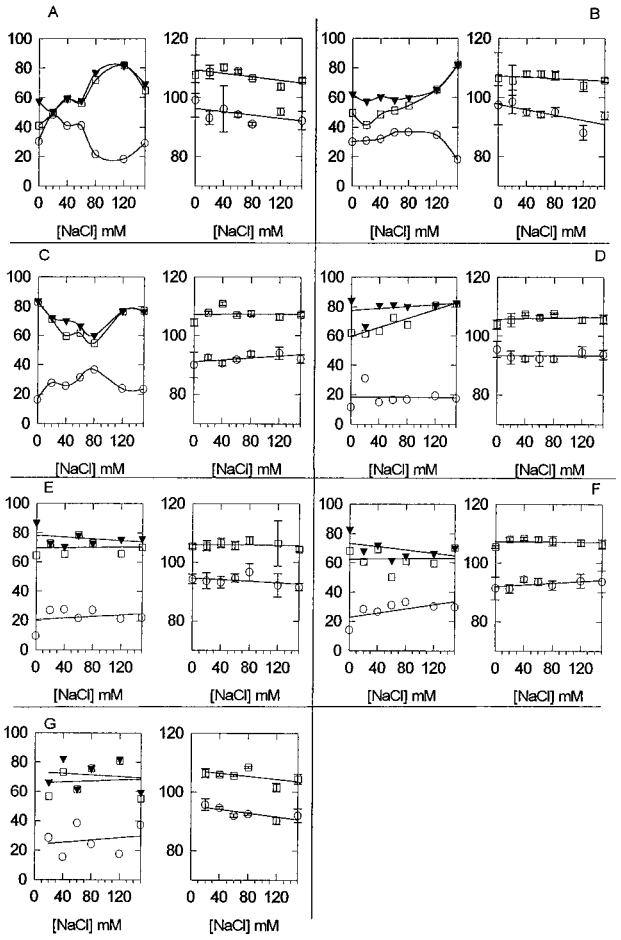

FIGURE 4: Condensation ratio (d) of chicken erythrocyte nuclei as a function of sodium chloride for different magnesium chloride concentrations: (A) 50, (B) 100, (C) 200, (D) 400, (E) 600, (F) 800, and (G) 800 μM. Same symbols as in Figure 3. Vertical bars are the confidence interval on the temperature parameter.

nucleotides, that is partially neutralized by the basic histone H1, resulting in a reduction of the negative charge of the phosphates $\theta_{II} = 0.58$ (Clark & Kimura, 1990). In chicken erythrocyte chromatin, $N_I = 92$ and $N_{II} = 40$ (Thomas, 1984; Van Holde, 1988). Domain III is core DNA, is composed of $N_{III} = 292$ bases, and has a fraction of phosphate charges neutralized by core histones $\theta_{III} = 0.447$ (Clark & Kimura, 1990). The molar fractions χ_{Domain} of nucleotides in a domain are

$$\chi_{Domain} = \frac{N_{Domain}}{N_I + N_{II} + N_{III}} \quad (3)$$

where the subscript Domain is I, II, or III. The electrostatic contribution $\Delta G°_{Ionic}$ to the chromatin condensation free energy per nucleotide is thus

$$\Delta G°_{Ionic} = \chi_I \Delta G°_{Bending} + \chi_I \Delta G°_I + \chi_{II} \Delta G°_{II} + \chi_{III} \Delta G°_{III} \quad (4)$$

Domain I has a contribution due to the free energy $\Delta G°_{Bending}$ required to bend a linker in condensed chromatin fiber. From eqs 3 and 6 in Fenley et al. (1992), it can be deduced that the bending free energy of DNA is equal to

$$\Delta G°_{Bending} = \frac{1}{4\pi\epsilon_0\epsilon_r} q^2_I F_1(R) \quad (5)$$

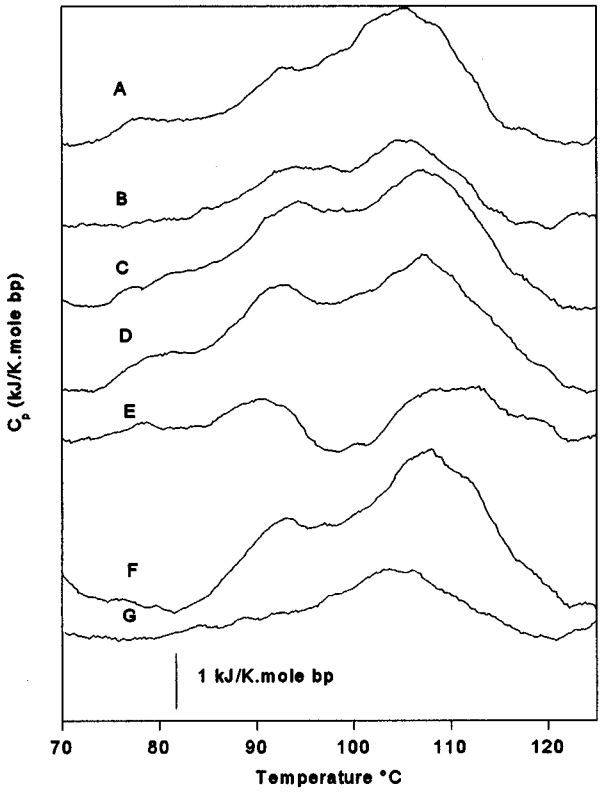

FIGURE 5: Differential scanning calorimetry thermograms of chicken erythrocytes nuclei in DM in the presence of 200 μM $MgCl_2$ and NaCl (A) 150, (B) 120, (C) 80, (D) 60, (E) 40, (F) 20, and (G) 1 mM.

where q^2_I is the phosphate charge of the linker and $F_1(R)$ is a geometrical factor depending on the radius R of bending of the DNA. In order to condense chromatin, it is necessary to decrease the distance between negatively charged DNAs of the nucleosomes of successive turns of the fiber, thus resulting in a free energy of electrostatic repulsion between phosphates of domains I, II, and III: $\Delta G°_I$, $\Delta G°_{II}$, and $\Delta G°_{III}$, respectively. From general electrostatic considerations (Stratton, 1941), the free energy of electrostatic repulsion between two DNA fragments of length L_1 and L_2 and of charge q_1 and q_2 is given by

$$\Delta G°_n = \frac{q_1 q_2}{4\pi\epsilon_0\epsilon_r} \int_0^{L_1} \int_0^{L_2} \frac{dl_1 dl_2}{L_1 L_2 r_{12}} = \frac{q_1 q_2}{4\pi\epsilon_0\epsilon_r} F_2(D_n) \quad (6)$$

where n = I, II, or III, r_{12} is the distance between the element dl_1 and dl_2. The integral term depends on the exact geometry of the system and has been collected in a geometrical factor $F_2(D_n)$ depending on the distance D_n between the DNA fragments in domains n. Combining eqs 4−6, one obtains

$$\Delta G°_{Ionic} = \frac{1}{4\pi\epsilon_0\epsilon_r} (\chi_I q^2_I \langle F_1(R_I)\rangle + \chi_I q^2_I \langle F_2(D_I)\rangle + \chi_{II} q^2_{II} \langle F_2(D_{II})\rangle + \chi_{III} q^2_{III} \langle F_2(D_{III})\rangle \quad (7)$$

Since the structure of the chromatin is not perfectly regular, it is necessary to use average geometrical factors $\langle F(R)\rangle$ and $\langle F(D)\rangle$ to take into account the local geometrical variations. As a first approximation, we shall assume that, on average, the factors $\langle F\rangle$ should be equal for each domain (We are developing a model describing the condensed structure of chromatin and carrying out numerical computations of the

different geometrical factors in order to avoid this approximation). Equation 7 can thus be approximated by

$$\Delta G^{\circ}_{\text{Ionic}} = \frac{\langle F \rangle}{4\pi\epsilon_0\epsilon_r} q^2_{\text{Tot}} \tag{8}$$

where

$$q^2_{\text{Tot}} = [2q^2_{\text{I}}\chi_{\text{I}} + q^2_{\text{II}}\chi_{\text{II}} + q^2_{\text{III}}\chi_{\text{III}}] \tag{9}$$

with q_n the residual phosphate charge in domain n. q^2_{Tot} is not an average charge. From a physical point of view, it cannot even be defined as a charge (it is the sum of the square of charges, not of charges): this term is only a short way to indicate that the total free energy is the weighed sum of the electrostatic contributions from each domain. However, for concision, we will refer to q^2_{Tot} as the "total square charge". $\langle F \rangle$ is a geometrical factor that depends on the exact positions of the interacting charges (units, m^{-1}), ϵ_0 is the vacuum permittivity, and ϵ_r is the dielectric constant of the medium. The double contribution of domain I (bending and electrostatic repulsion) to the total free energy is taken into account by the factor 2 in the first term of eq 9. The residual charge q_n (n = I, II, or III) on a DNA domain is equal to

$$q_n = q(1 - \theta_{\text{Na}} - N\theta_{\text{M}} - \theta_n) \tag{10}$$

where q is the proton charge, θ_n is the fraction of charge neutralized by the proteins in the domain (n = I, II, or III), N is the charge of the cation M^{N+}. θ_{Na} and $N\theta_{\text{M}}$ are the fractions of charge neutralized, respectively, by sodium and multivalent cation that are computed in each domain using the Manning theory. The equations were adapted from eqs 53 and 54 in Manning (1978) in order to account for the charge neutralized by the histones.

Salt-Induced Chromatin Condensation Is Predicted To Be an Entropy-Driven Process. Two opposing forces are controlling the transfer of a cation from the bulk solution to the DNA surface (Manning, 1978): (1) the favorable reduction of the electrostatic repulsion between adjacent phosphate charges on the DNA and (2) the unfavorable entropic decrease resulting from the diffusion of cations from bulk solution to "bound" state of locally higher concentration. As the amount of bound cations is mainly driven by the entropic term and chromatin condensation is controlled mainly by the electrostatic repulsion between phosphate groups, which is dependent on the cation "binding", chromatin condensation is predicted to be an entropy-driven process; that is exactly what is experimentally observed. We are now going to show that our model offers a unified interpretation of DSC measurements and of several observations from the literature.

The Model Predicts the Salt Dependence of the Condensation Ratio. The change of q^2_{Tot} as a function of cation concentration is represented in Figure 6A. As the cation concentration increases, the residual phosphate charge decreases. Furthermore, the greater the cation charge, the more important the phosphate charge reduction is for a given cation concentration. By reporting the cation concentration ranges inducing condensation (Figure 3) in Figure 6, it can be seen that condensation occurs when the total square charge is included in the gray zone of Figure 6. The central value of the zone (4.6×10^{-2} q^2 where q is the proton charge) will

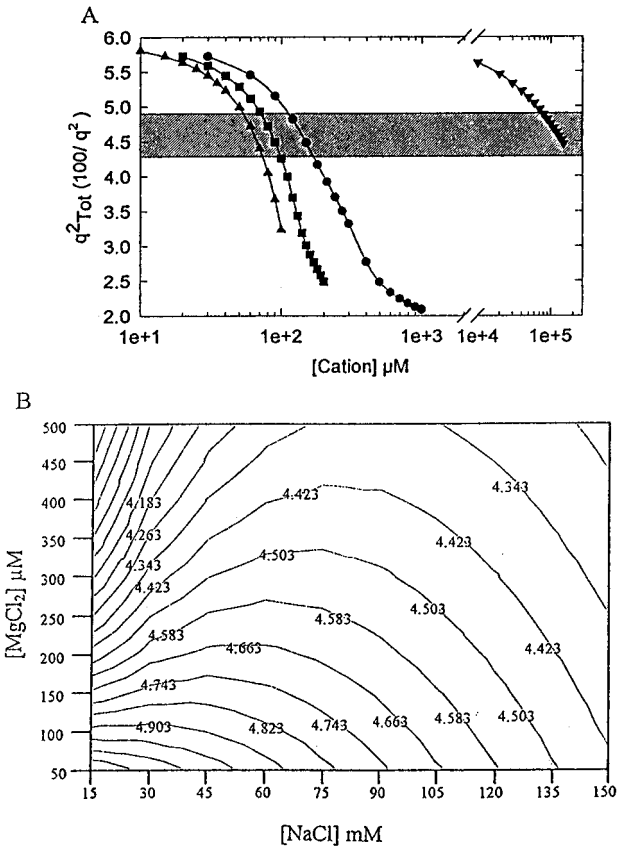

FIGURE 6: (A) Computed total square charge in chromatin as a function of cation concentration. (▲) tetravalent; (■) trivalent; (●) divalent; (▼) monovalent. Condensation occurs in the gray zone. (B) Computed total square charge as a function of both magnesium and sodium concentrations. Units are in 10^{-2} q^2.

be considered as the critical total square charge inducing condensation. As the structure of condensed chromatin fiber is independent of the chromatin origin (McGhee, 1983), the critical value of the total square charge can be expected to be independent of the chromatin type. However, the salt concentration required to reach this critical total square charge varies with chromatin type, depending on the length of the linker DNA. Indeed, for a given salt concentration, the residual charge in the linker domain (q_{I}) is higher than in other domains because of the absence of the positively charged histones. According to eq 9, it can thus be predicted that the longer the linker length (large χ_{I}), the higher the salt concentration required for condensation. As the linker length of sea urchin sperm, chicken erythrocyte, and rat liver chromatin are respectively 77, 44 and 30 bp long, we expect that the salt concentration required for condensation of these different chromatin types will decrease in the order sea urchin sperm > chicken erythrocyte > rat liver, which is what is actually observed experimentally (Koch et al., 1987; McGhee et al., 1983).

The observed competition effect between sodium and magnesium may be predicted on the basis of Figure 6. When the magnesium concentration is 200 μM, the total square charge first increases as the sodium concentration increases and then decreases above 75 mM NaCl.

In order to further verify the generality of the model, all the experimental data of Figures 3 and 4 were plotted versus the theoretically computed q^2_{Tot} (80 data points) in Figure 7. Combining eqs 2 and 8, we obtain

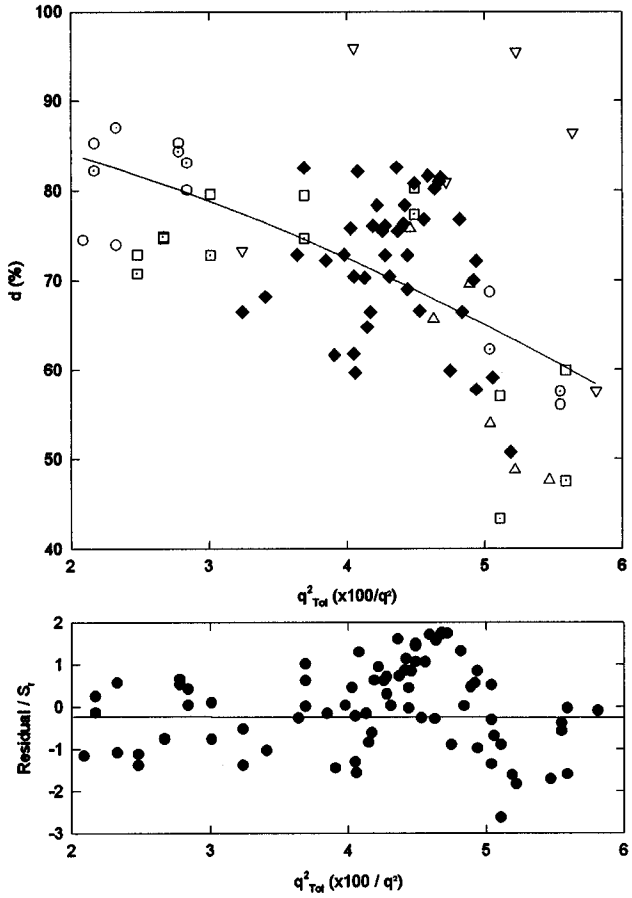

FIGURE 7: Condensation ratio versus the theoretically computed total square charge. All the data are collected from Figures 3 and 4. (○) $MgCl_2$; (□) $TbCl_3$; (⊡) spermidine^{3+}; (⊙) $MgCl_2$; (△) NaCl; (▽) spermine^{4+}; (◆) mixtures of $MgCl_2$ and NaCl. The line is the best regression through the data points. The residuals are shown at the bottom.

$$d = \frac{e^{aq^2_{Tot}+b}}{1 + e^{aq^2_{Tot}+b}} \qquad (11)$$

where $a = (-\langle F \rangle)/(4\pi\epsilon_0\epsilon_r kT)$ and $b = (-\Delta G_{Nonionic})/(kT)$. The parameters a and b in eq 11 are adjusted in order to get the best fit curve, also plotted in Figure 7. The residuals are randomly dispersed around the fitted curve (Figure 7, bottom) with a scatter lower than 2 standard deviations. Furthermore, the standard deviation of the fit (7.9%) is not significantly different from the experimental error on the data points (5%). The curve can thus be considered as a reasonable fit of the data points (Himmelblau, 1970). From Figure 7, it is clear that the value $q^2_{Tot} = 4.6 \times 10^{-2}\ q^2$ corresponds to a condensation ratio d of 68%, i.e., at midcondensation (condensation ratio varies from 50% to 80%).

The Model Predicts the Condensation Ratio Dependence on Chromatin Concentration. The previous observations (McGhee et al., 1980; Marquet et al., 1988) that, contrary to NaCl-induced chromatin condensation which is only dependent on cation concentration, the $MgCl_2$- or spermidine^{3+}-induced condensation is dependent on the ratio I/P = [cation]/[chromatin] may be explained by our model. The total square charge is predicted to be independent of the chromatin concentration in presence of monovalent cations (Figure 8A). For higher charge cations (Figure 8B,C), the total square charge depends on both cations and chromatin

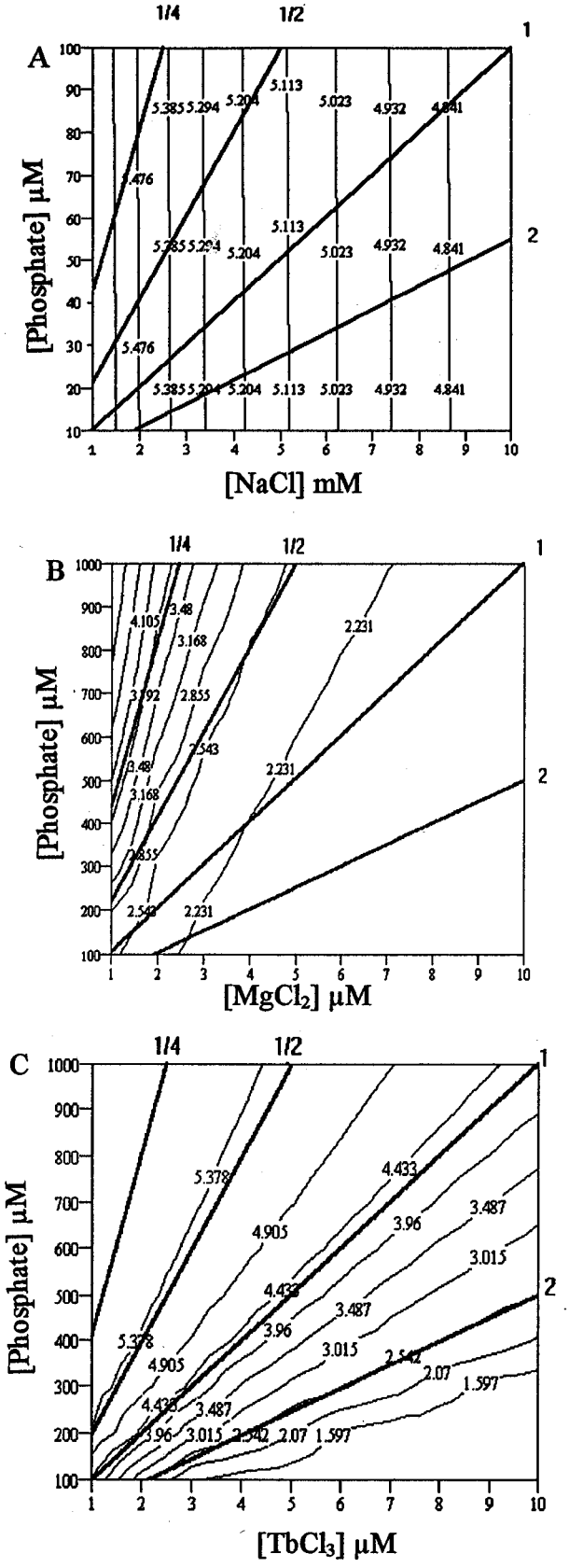

FIGURE 8: Computed total square charge (in $10^{-2}\ q^2$; light lines) as a function of chromatin (vertical axis) and cation concentrations (horizontal axis) for (A) monovalent cations, (B) divalent cations, and (C) trivalent cations. The bold lines represent iso-I/P lines.

concentrations. All the points at constant I/P are on a iso-I/P line (bold line). In presence of M^{2+} cation (Figure 8B), the condensation ratio is constant on a iso-I/P lines because

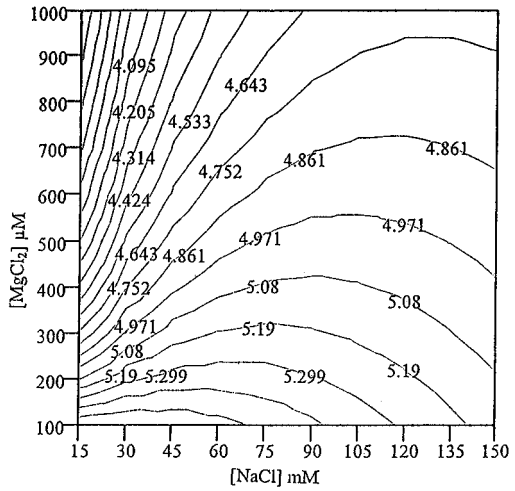

FIGURE 9: Computed total square charge (in $10^{-2}\ q^2$) in H1-depleted chromatin as a function of magnesium and sodium concentration.

they are parallel to the isocharge lines up to $I/P = 1/3$. Above $I/P = 1/3$, the iso-I/P lines cross isocharge lines but in a region where chromatin is in its totally condensed state anyway ($q^2_{Tot} < 4.6 \times 10^{-2}\ q^2$). In the case of M^{3+} cations (Figure 8C), all the iso-I/P lines are parallel to the isocharge lines. For high charge cations, the condensation is thus predicted to be only dependent on the I/P ratio.

The Model Predicts the Salt Dependence of the H1-Depleted Chromatin Condensation. H1-depleted chromatin can no longer be condensed as completely as normal chromatin at high ionic strength with monovalent cations (Butler, 1980; Ausio et al., 1986; Thoma et al., 1979). However Jin and Cole (1986) observed that magnesium cations still induce chromatin condensation but at a higher concentration and postulated the existence of a cross-link between DNA fibers by multivalent cations, as already proposed by Ausio et al. (1986). In fact, it is possible to explain the observations by the polyelectrolyte counterion condensation theory without assuming the existence of hypothetical cross-links. In our simple chromatin model, the parameters become $N_I = 132$ and $N_{II} = 0$ when H1 has been removed. Figure 9 shows the total square charge computed with these new parameters. It is clear that at low magnesium concentrations, sodium cations cannot decrease the charge density below the critical limit of 4.6×10^{-2} q^2. A concentration of 350 μM magnesium is necessary to reach the critical $4.6 \times 10^{-2}\ q^2$, in agreement with the observations.

The Model Predicts the H1-Induced Chromatin Condensation. Below 20 mM NaCl (Clark & Thomas, 1986), H1 binding to DNA is a non-cooperative process, but it is cooperative above 50 mM NaCl with null binding enthalpy (Watanabe, 1986). If one neglects complications due to the inter-histone interactions, the binding results principally from an electrostatic interaction between DNA and the protein (Watanabe, 1986). On the other hand, the binding of H1 to chromatin is a non-cooperative process, as shown by sedimentation analysis (Allan et al., 1981) and DSC studies (Russo et al., 1995). A contradictory report (Watanabe, 1984) of a cooperative process is due to the reconstitution technique used that did not preserve the nucleosome repeat (Russo et al., 1995). Cooperativity in H1 binding to chromatin is unlikely because it occurs at independent sites, and there cannot be inter-histone interactions between globular parts as they are used to seal the chromatosome. Russo et al. (1995) have measured by DSC the H1-induced condensation of H1-depleted calf thymus chromatin and showed that the free energy of condensation can be empirically related to the amount of H1 molecule bound on the chromatin by

$$\Delta G^\circ_{Cond} = \Delta G^\circ_c + \Phi(R)\Delta G^{int} \qquad (12)$$

where ΔG°_c is the free energy required to form the condensed state in the absence of H1 and ΔG^{int} is the free energy change resulting from the interaction between H1-bound nucleosomes. $\Phi_c(R)$, the fraction of H1-containing nucleosomes that is interacting, is equal to

$$\Phi_c(R) = \sum_{k=c}^{\infty} kR^k(1-R)^2$$

where c is the minimal size of a cluster of nucleosomes that can form stabilizing interactions and R is the fraction of nucleosomes that is occupied by H1 molecules. For c superior to 1, chromatin condensation is cooperative. Russo et al. found a value of $c = 2$, thus only a very slightly cooperative process.

The use of polyelectrolyte theory in this case is justified because H1 binding to DNA and chromatin was reported to be essentially an electrostatic process (Watanabe, 1986; Kumar & Walker, 1980). In our model, the fraction of nucleotides in domain I (χ'_I) and domain II (χ'_{II}), when only a fraction R of the H1 are bound are respectively

$$\chi'_I = \chi_I + (1-R)\chi_{II}$$

$$\chi'_{II} = R\chi_I$$

Introducing them into eqs 2 and 4 gives

$$\Delta G^\circ_{Cond} = \Delta G_1 + R\Delta G_2 \qquad (13)$$

with

$$\Delta G_1 = N_{Nucl}(\Delta G_{NonIonic} + (\chi_I + \chi_{II})(\Delta G^\circ_{Bending} + \Delta G^\circ_I) + \chi_{III}\Delta G^\circ_{III})$$

$$\Delta G_2 = \chi_{II} N_{Nucl}(\Delta G^\circ_{II} - \Delta G^\circ_{Bending} - \Delta G^\circ_I) \qquad (14)$$

where N_{Nucl} is the number of nucleotides in a nucleosome; ΔG_1 is the electrostatic free energy of condensation of a chromatin totally depleted of H1; and ΔG_2 is the change of electrostatic free energy in domain II due to neutralization by H1. Fitting the Russo data with eq 13, one gets $\Delta G_1 =$ 9.9 kJ/mol of nucleosome and $\Delta G_2 = -23.0$ kJ/mol of nucleosome. ΔG_1 is positive because the condensation of chromatin in the absence of H1 is not a thermodynamically favorable process and ΔG_2 is negative because the repulsion between the negatively charged linker DNAs is reduced by the positive histone. Now, remembering that

$$\Phi_1(R) = \sum_{k=1}^{\infty} kR^k(1-R)^2$$
$$= (1-R)^2 R \sum_{k=1}^{\infty} kR^{k-1}$$
$$= (1-R)^2 R \frac{1}{(1-R)^2}$$
$$= R$$

and comparing the condensation free energy in both theories (eqs 12 and 13), it is obvious that $\Delta G_1 = \Delta G^\circ_c$ and $\Delta G_2 = \Delta G^{int}$. So the empirical relation 12 can be interpreted in terms of the polyelectrolyte theory provided that H1-induced condensation is a non-cooperative process ($c = 1$), which is the case.

ACKNOWLEDGMENT

We would like to thank Prof. E. Patrone and Dr. C. Balbi and their teams for their helpful advice about DSC.

REFERENCES

Allan, J., Cowling, G. J., Harborne, N., Cattini, P., Craigie, R., & Gould, H. (1981) *J. Cell Biol. 90*, 279−288.
Ausio, J., Sasi, R., & Fasman, D. (1986) *Biochemistry 25*, 1981−1988.
Balbi, C., Abelmoschi, M. L., Gogioso, L., Parodi, S., Barboro, P., Cavazza, B., & Patrone, E. (1989) *Biochemistry 28*, 3220−3227.
Barboro, P., Pasini, A., Parodi, S., Balbi, C., Cavazza, B., Allera, C., Lazzarini, G., & Patrone, E. (1993) *Biophys. J. 65*, 1690−1699.
Bartolomé, S., Bermudez, A., & Daban, J. R. (1994) *J. Cell Sci. 107*, 2983−2992.
Bates, D. L., Butler, G., Pearson, C., & Thomas, J. O. (1981) *Eur. J. Biochem. 119*, 469−476.
Butler, P. J. G. (1980) *J. Mol. Biol. 140*, 505−529.
Cavazza, B., Brizzolara, G., Lazzarini, G., Patrone, E., Piccardo, M., Barboro, P., Parodi, S., Pasini, A., & Balbi, C. (1991) *Biochemistry 30*, 9060−9072.
Clark, D. J., & Thomas, J. O. (1986) *J. Mol. Biol. 187*, 569−580.
Clark, D. J., & Kimura, T. (1990) *J. Mol. Biol. 211*, 883−896.
Fenley, M. O., Manning, G. S., & Olson, W. K. (1990) *Biopolymers 30*, 1191−1203.
Fenley, M. O., Manning, G. S., & Olson, W. K. (1992) *J. Chem. Phys. 96*, 3963−3969.
Finch, J. T., & Klug, A. (1976) *Proc. Natl. Acad. Sci. U.S.A. 73*, 1897−1901.
Flock, S., Labarbe, R., & Houssier, C. (1995) *J. Biomol. Struct. Dyn. 13*, 87−102.
Fogolari, F., Cattarinussi, S., Esposito, G., & Viglino, P. (1993) *J. Biomol. Struct. Dyn. 11*, 629−635.
Himmelblau, D. M. (1970) in *Process analysis by statistical methods*, Wiley & Sons, New York.
Jayaram, B., Sharp, K. A., & Honig, B. (1989) *Biopolymers 28*, 975−993.
Jin, Y., & Cole, R. D. (1986) *J. Biol. Chem. 261*, 15805−15812.
Koch, M. H. J., Vega, M. C., Sayers, Z., Michon, A. M. (1987) *Eur. Biophys. J. 14*, 307−319.
Kumar, N. M., & Walker, I. O. (1980) *Nucleic Acids Res. 8*, 3535−3550.
Labarbe, R., Mignon, S., Flock, S., & Houssier, C. (1996) *J. Fluoresc.* (in press).
Le Bret, M., & Zimm, B. H. (1984) *Biopolymers 23*, 271−285.
Manning, G. S. (1978) *Q. Rev. Biophys. 11*, 179−246.
Manning, G., Ebralidse, K. K., Mirzabekov, A. D., & Rich, A. (1989) *J. Biomol. Struct. Dyn. 6*, 877−889.
Marquet, R., & Houssier, C. (1991) *J. Biomol. Struct. Dyn. 9*, 159−167.
Marquet, R., Colson, P., Matton, A. M., & Houssier, C. (1988) *J. Biomol. Struct. Dyn. 5*, 839−857.
McGhee, J. D., Rau, D. C., Charney, E., & Felsenfeld, G. (1980) *Cell 22*, 87−96.
McGhee, J. D., Nickol, J. M., Felsenfeld, G., & Rau, D. C. (1983) *Cell 33*, 831−841.
Rajasekaran, E., & Jayaram, B. (1994) *Biopolymers 34*, 443−445.
Russo, I., Alberti, I., Parodi, S., Balbi, C., Allera, C., Lazzarini, G., & Patrone, E. (1995) *Biochemistry 34*, 301−311.
Stratton, J. A. (1941) in *Electromagnetic Theory*, Mc Graw-Hill, New York.
Subirana, J. A. (1992) *FEBS Lett. 302*, 105−107.
Thoma, F., Koller, T., & Klug, A. (1979) *J. Cell Biol. 83*, 403−427.
Thomas, J. O. (1984) *J. Cell Sci. Suppl. I*, 1−20.
Thomas, J. O., & Khabaza, J. A. (1980) *Eur. J. Biochem. 112*, 501−511.
Thomas, J. O., & Rees, C. (1983) *Eur. J. Biochem. 134*, 109−115.
Touchette, N. A., & Cole, R. D. (1985) *Proc. Natl. Acad. Sci. U.S.A. 82*, 2642−2646.
Touchette, N. A., & Cole, R. D. (1992) *Biochemistry 31*, 1842−1849.
Van Holde, K. E. (1988) in *Chromatin*, Springer-Verlag, New York.
Watanabe, F. (1984) *FEBS Lett. 170*, 19−22.
Watanabe, F. (1986) *Nucleic Acids Res. 14*, 3573−3585.
Widom, J. (1986) *J. Mol. Biol. 190*, 411−424.
Widom, J. (1989) *Annu. Rev. Biophys. Biophys. Chem. 18*, 365−395.
Zlatanova, J., Leuba, S. H., Yang., G., Bustamante, C., & Van Holde, K. E. (1994) *Proc. Natl. Acad. Sci. U.S.A. 91*, 5277−5280.

BI951636J